Macromolecules
Cite This: Macromolecules 2019, 52, 9620−9631
Article
pubs.acs.org/Macromolecules

The "Superlubricity State" of Carbonaceous Fillers on Polyethylene-Based Composites in a Molten State

Eder. H. C. Ferreira, Ricardo. J. E. Andrade, and Guilhermino J. M. Fechine*

Mackenzie Institute for Research in Graphene and Nanotechnologies − MackGraphe, Mackenzie Presbyterian University, Rua da Consolação 896, São Paulo, SP 01302-907, Brazil

Supporting Information

ABSTRACT: It is very well known that the incorporation of fillers into polymers increases their viscosity in a molten state; however, results contrary to this have been reported when graphite (Gr), graphite oxide (GrO), and graphene oxide (GO) among other carbonaceous fillers are used. Many authors have justified the reduction in polymer viscosity due to the slipping interlayers of the Gr, GrO, and GO fillers. The slipping interlayer cannot explain the reduction in polymer viscosity since the shear stresses produced or applied during rheological tests are lower than the interlayer shear strength of these fillers. Here, rheological experiments with two types of polyethylenes and Gr, GrO, and GO as fillers were carried out to elucidate this phenomenon. Remarkably, it was observed that the viscosity reduction occurs due to the presence of agglomerates in the composites. The agglomerates contain many flake−flake contacts out of registry (superlubricity state), which have very low slipping resistance. The slipping of these contacts promotes the reduction in polymer viscosity during rheological tests. The elucidation of the superlubricity state phenomenon proposed here may contribute to the understanding of the carbonaceous filler influence during the deformation of polymer composites.

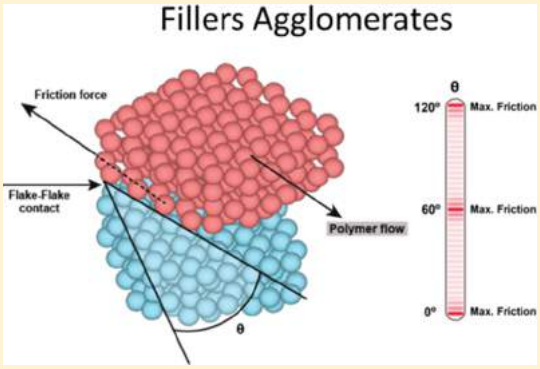

INTRODUCTION

Many publications have shown that the incorporation of nanofillers or fillers in molten polymers strongly increase their viscosity.[1−5] This observation was predicted by Einstein in 1906, when he demonstrated that, for an empirical linear expression, the viscosity of a fluid increases with the immiscible particle volume fraction added.[6] However, some publications have observed the opposite results when fillers are added to the polymers. An example of this is the manuscript entitled "Nanoscale effects leading to non-Einstein-like decrease in viscosity" published in 2003 by Mackay and co-authors.[7] They observed that the incorporation of cross-linked polystyrene (PS) nanoparticles to linear polystyrene reduced the viscosity of the polymer during rheological tests in an oscillatory flow. They attributed the nanoparticle confinement phenomenon (increase free volume induced around the nanoparticle) as the cause for the reduction in polymer viscosity.[7]

Similarly, results have been observed for polymeric composites filled with single-walled carbon nanotubes (SWNT)[8] and silica nanoparticles[9] and prepared using solution mixing.[8,9] In this case, the reduction in viscosity is not attributed to the nanoparticle confinement phenomenon but to the "selective adsorption" of chains with higher molecular weight by fillers during crystallization or precipitation from solution.[8,9]

Both these explanations support the case that the nanoparticle confinement phenomenon is possible or selective absorption is possible when the composites and nanocomposites are prepared from solution mixing. When the composites are prepared by melt mixing and microparticles are added, neither explanations are appropriate.

Two decades earlier, Yip et al. and Kazatchkov et al. had already reported that platelet-like fillers could act as a lubricant additive during a melt polymer flow. Specifically, they showed that boron nitride could promote the reduction of storage (G') and loss (G'') moduli and act as a processing aid, eliminating melt fracture and reducing the head pressure in the extrusion blow molding operation.[10,11]

Recently, other authors have studied filled polymers with carbonaceous materials, and they have demonstrated the lubricating actions of these fillers during the melt polymer flow. They have reported, using rheological test in an oscillatory flow or steady shear flow, that the viscosity and G' and G'' moduli can be reduced when graphite (Gr), graphene oxide (GO), and carbon nanotubes (CNT) are added.[12−17] However, it is intriguing that other authors using the same polymers have observed increases in viscosity when the same carbonaceous filler types were added.[3,4,16,18] The main explanations given for the viscosity reduction with the addition of these fillers are that during the rheological test, the layer stacking structure and the poor interlayer interaction of these fillers (graphite and graphene

Received: August 20, 2019
Revised: December 2, 2019
Published: December 16, 2019

DOI: 10.1021/acs.macromol.9b01746
Macromolecules 2019, 52, 9620−9631

oxide) favor the easy interlayer slip, leading to the reduction in the polymer viscosity.[12,13,17] However, the interlayer high shear strength values of graphite (Gr, 0.2 MPa to 7 GPa),[19] graphite oxide (GrO, 5.3 ± 3.2 MPa),[20] and graphene oxide (GO, 0.54−4.48 GPa)[21] reported make this explanation inconsistent since the shear stress applied during rheological tests are not able to reach these values. The high values of shear strength reported are due to AB stacking layers of graphite and preserved AB stacking regions of graphite oxide and graphene oxide after oxidation (even to a high oxidation degree).[22−24] AB stacking layers have high symmetry of the individual atoms, which promotes continuous interactions between all the atoms of the lattice during slipping, causing stick−slip motion.[19] The interactions of the atoms cause high static friction (stick), justifying the high shear strength values.[19] In the case of the graphite oxide and graphene oxide, the interaction between functional groups (Coulombic, van der Waals, and H-bonding contribution) also causes the stick−slip motion and very high friction, which strongly contributes to a high interlayer shear strength of these fillers.[20,21,25−28]

In addition, if easy sliding occurs between stacking layers, how have other publications that studied the same composites with carbonaceous not observed the same phenomenon? Instead, they observed increased viscosity. This demonstrates that the slipping between the stacking structure of fillers is clearly not an adequate explanation for these cases. Here, for the first time, to the best knowledge of the authors, a new approach to elucidate the superlubricity phenomenon is taken.[29] Hirano and Shinjo suggested that two crystalline lattices at contact out of registry (incommensurate contact) led to disappearance of friction, superlubricity state.[29] This fundamental concept will be used to understand the phenomena presented. Here, based on the rheological testing of the composites, it will be shown that the carbonaceous filler agglomerates present in the polymers can present superlubricity and drastically influence the rheological properties of the polymers.

To contribute to the understanding of viscosity reduction of filled polymers, the action mechanism of carbonaceous fillers (Gr, GrO, and GO) on the rheological properties of polyethylene with different molecular weights will be evaluated. In this study, the lubricant effect attributed to these fillers in the steady shear viscosity behavior, creep behavior, and linear viscoelastic properties of high-molecular-weight polyethylene (HMWPE) and high-density polyethylene (HDPE) polymers were evaluated. Two different commercial PEs were chosen to have a very similar interface, while the viscosities are very distinct. At the same time, two filler contents are used, 0.1 and 5.0 wt %, to have one composition with a well-dispersed filler (exfoliated) and the other one with a higher presence of agglomerates. Both scenarios can help elucidate the real effect of the carbonaceous fillers with 2D and 3D shapes on the rheology of polymers.

EXPERIMENTAL SECTION

Preparation and Characterization of Graphite Oxide (GrO) and Multilayer Graphene Oxide (mGO). The graphite (Gr) used was provided by Sigma-Aldrich with 99.9% purity and particle size less than 45 μm. First, the graphite oxide was prepared following a modified Hummer's method.[30] Graphite oxide (GrO, 100 mg) was exfoliated in deionized water using an ultrasonic bath (Elma, P30) for 40 min in individual 100 mL batches to obtain a 1 mg mL^{-1} mGO suspension. The denomination mGO is used here due to the number of GO layers obtained, as shown later.

Characterization of Fillers. *Raman Confocal Microscopy.* Spectra of graphite and GrO were acquired using a WITec Alpha300R confocal Raman spectrometer. The excitation source was a 532 nm laser.

Thermogravimetric Analysis (TGA). The thermal stability of graphite and graphite oxide was evaluated using thermogravimetric analysis (DSC/TGA Q600, TA Instruments). All measurements were conducted under an inert atmosphere (nitrogen) over a temperature range of 30−1000 °C. A second experiment was carried out to check the possibility of GrO thermal reduction during the processing and rheological test. This experiment was conducted under an inert atmosphere over a temperature range of 30−200 °C (10 °C min^{-1}), and after reaching the final temperature, an isotherm was kept for 120 min.

X-ray Diffraction Analysis. Analysis of graphite and GrO were performed in a Rigaku diffractometer with Cu Kα radiation (λ = 1.42 Å). The scan range used was from 5 to 70° at a scan rate of 0.083° s^{-1}.

Scanning Electron Microscopy (SEM). SEM imaging was performed on a JEOL JSM-6510 at 25 KeV.

Atomic Force Microscopy (AFM). Drop casting of mGO dispersion was prepared on top of fresh mica and analyzed in an Icon Dimension (Bruker) equipped with RTESPA.

Fourier Transform Infrared Spectrophotometer-Attenuated Total Reflection. Analyses of graphite and GrO were performed in a Shimadzu IRAffinity-1S. The spectroscopy range used was 500 to 4000 cm^{-1}. The resolution used was 4 cm^{-1}.

Processing and Characterization of Composites. *Two Commercial PEs with Different Molecular Weights Were Used.* HMWPE and HDPE with a melt mass-flow rate (190 °C/21.6 kg) of 0.70 and 10 g/10 min, respectively. The HMWPE is a linear polyethylene obtained by Ziegler's catalytic system and presenting a density of about 0.951 g cm^{-3}. The number-average molecular weight ($\bar{M}_n$) values of the neat polymer, HMWPE and HDPE, are 1.48 × 10^5 g mol^{-1} and 7.26 × 10^4 g mol^{-1}, respectively. The polydispersity index (PDI) values for HMWPE and HDPE are 1.84 and 2.32, respectively. Both polymers were supplied by Braskem; there is no mention of the presence of stabilizers on them.

Processing of Nanocomposites. First, the polyethylene powders were recovered from the graphene oxide, graphite oxide, and graphite using a solid−solid deposition strategy, which is performed in a rotary evaporator.[12] The mixing process intended to obtain composites with the following final contents: 0.1 and 5 wt % GO, GrO, and Gr when incorporated into HMWPE and 5 wt % GO, GrO, and Gr for HDPE. Afterward, the recovered powders were processed in a twin-screw extruder L/D = 40 having a barrel bore diameter and screw diameter of 11 mm (Process 11, Thermo Scientific) at a screw speed of 150 rpm, operating with a temperature profile in zone 1 at 115 °C, zone 2 at 170 °C, and zones 3−7 at 200 °C, and die at 200 °C, operating with a feed rate of 3 g min^{-1}. The HMWPE and its composites, due to its high viscosity, were processed without the extrusion die, making the processing of these materials possible. HMWPE (fillers, 0.1 and 5 wt %) and HDPE (fillers, 5 wt %) specimens were molded in a hot hydraulic press (Solab, SL-1220), operating at a temperature of 200 °C on the top and bottom plate, and subjected to 4 tons of pressure for 10 min. The samples were cooled at room temperature.

X-ray Microtomography. Pieces at least 2 mm × 2 mm × 1.2 mm from rheology specimens were used for this characterization. Samples were analyzed in a SkyScanner 1272 (Bruker), using 20 kV and 175 μA X-ray source, with a final image resolution of 2 μm/pixel.

Optical Microscopy. 28 Eclipse LV100ND with the aid of NIS-Element software. The agglomerate particle counts were performed on six different regions of the sample with 100× amplification in the transmission mode. In total, there were 30−60 counts.

Transmission Electron Microscopy (TEM). TEM imaging was performed on a Tecnai G2-20 FEI SuperTwin microscope at 200 kV. Ultramicrotomed samples with 60 nm thickness were collected on top of 200 mesh copper grids.

Size Exclusion Chromatography Analysis. Molecular weight and its distribution were measured using a size exclusion chromatography (Malvern) equipped with a refractive index detector. All samples were analyzed in trichlorobenzene (TBT) at 140 °C with 0.25% butylated

DOI: 10.1021/acs.macromol.9b01746
Macromolecules 2019, 52, 9620−9631

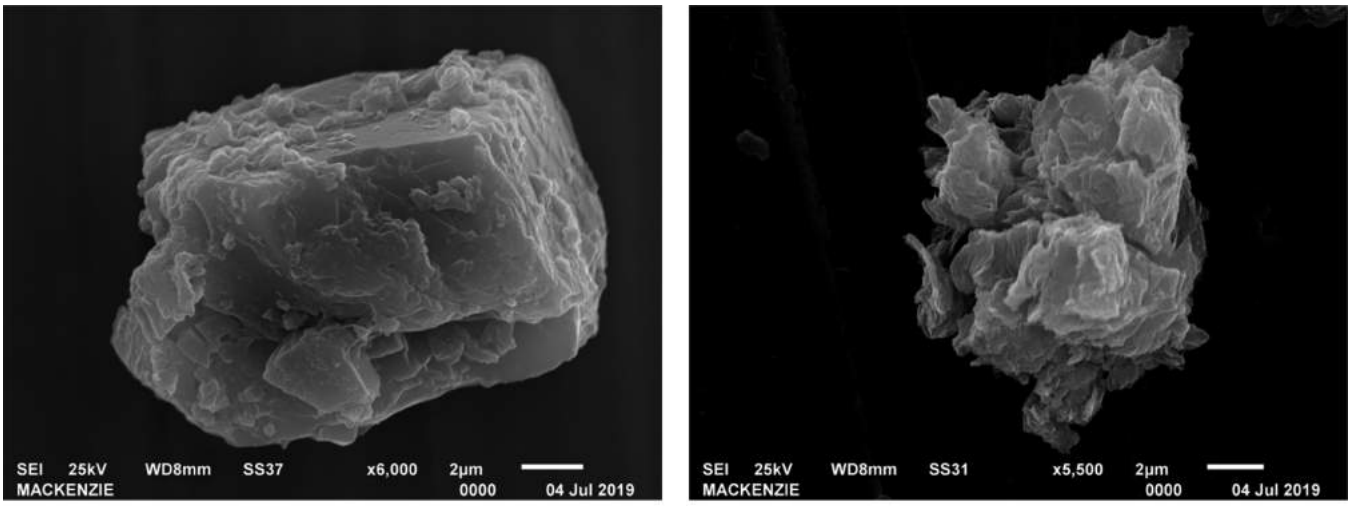

Figure 1. Scanning electron microscopy (SEM) images of (a) graphite and (b) graphite oxide.

hydroxytoluene. A 1 mL min^{-1} solvent flow was used in both pumps, and calibration was performed using mixed PS standards (Poly-Analytik) from 1.5 kDa to 4 MDa.

Rheological Test in Oscillatory Flow (Anton Paar 102 Rheometer). The test was conducted using plate/plate geometry, at 200 ° C, with an angular velocity of 0.01 to 100 rad s^{-1} and a deformation of 1% (within the linear viscoelasticity regime) under an inert atmosphere. The samples were left in thermal equilibrium for 15 min before the start of the test, and the time test was 2 h.

Rheological Test in Steady Shear Flow (Anton Paar 102 Rheometer). Analyses of steady shear viscosity versus the shear rate of the polymers and composites were performed using plate/plate geometry, with a 1.2 mm gap, 200 °C, and a shear rate from 10^{-4} to 1 s^{-1} for HMWPE and its composites and from 10^{-4} to 100 s^{-1} for HDPE and its composites for 30 min under an inert atmosphere. The lower shear rates used for HMWPE and its composites were because of the high flow resistance (viscosity) for this polymer. The highest shear rate used exceeded the capacity of the rheometer. Creep testing was performed at 200 ° C, with a shear stress of 500 and 10 Pa for 10 min under an inert atmosphere.

RESULTS AND DISCUSSION

Discussion Based on the Superlubricity State of Graphite, Graphite Oxide, and Multilayer Graphene Oxide. Graphite (Gr) and graphite oxide (GrO) were characterized using X-ray diffraction (Figure 1S), Raman spectroscopy (Figure 2S), thermogravimetry (Figure 3S), and infrared spectroscopy (Figure 4S). All results are presented in the Supporting Information.

The presence of the AB stacking region and interlayer functional groups (epoxy, carboxyl, and hydroxyl) are responsible for the stick−slip phenomenon observed in the particles produced here (GrO and mGO), as can be seen in the Supporting Information. X-ray diffractograms (Figure 1S) show the permanence of the 26 and 42° peaks of graphite after oxidation (GrO), indicating that a fraction of AB stacking is still preserved in the graphite oxide structure. In the infrared spectra (Figure 4S), the carboxyl, carbonyl, hydroxyl, and epoxy groups inserted in graphite due to oxidation are shown, as well as evidence of nonoxidized regions (C═C bond). Therefore, due to the characteristics of the mGO and GrO produced here, their interlayer shear stress values must have the same order of magnitude as those already reported in specialized publications.[19−21] However, the slipping interlayer phenomenon of mGO and GrO is not adequate to explain the filled polymer viscosity reduction results that will be presented later.

Dienwiebel et al. have argued the "easy interlayer slipping" explanation to justify the good lubricating properties of graphite, which is unsatisfactory. Dienwiebel et al. have attributed the good lubricating properties of graphite to the large fraction of the out-of-registry contacts (incommensurate contacts) possible between graphite flakes (flake−flake contact), while only a small fraction of contacts will present high friction due to perfectly aligned (in registry) lattices of flakes, causing stick−slip phenomenon.[31−33] The incommensurate contacts correspond to the greater probability of orientation between the layers of flakes at contact. They correspond to the all angular orientation within the intervals of 60°, which the "superlubricity state" will be present. These angular orientations prevent a collective stick−slip motion between the interface atoms in contact during slipping.[31−33] While the contacts in registry (commensurate contact) correspond only to the orientations of planes within 60° spacing (AB or AA stacking).[31−34] The superlubricity phenomenon was also observed for molybdenum disulfide, carbon nanotubes, and mica also due to the slipping of incommensurate contacts.[29,35,36]

Based on the results presented by Dienwiebel et al., the amount of flake−flake contacts available to slip will influence the intensity of the lubricating behavior of the fillers. The oxidation (after Hummer's method) of the graphite causes a strong fragmentation of flakes.[22,23,37] This can be noted in Figure 1 a,b where the graphite oxide (Figure 1b) has smaller flakes than the Gr (Figure 1a). Data presented in the Supporting Information shows the intensity of the Gr fragmentation based on the reduction of crystal size after oxidation. The calculations were made based on the data obtained from X-ray analyses (Figure 1S) and Raman confocal microscopy analyses (Figure 2S).

However, it is expected that lubricant behavior of GrO is higher than the Gr. The smaller size of the GrO flakes provides a larger amount of flake−flake contacts (incommensurate contacts) available to slip; consequently, a higher lubricant effect is expected during the rheological test of composites.

After the exfoliation of GrO in a water medium to obtain the mGO, the flake size reduces drastically. Figure 2 shows

DOI: 10.1021/acs.macromol.9b01746
Macromolecules 2019, 52, 9620−9631

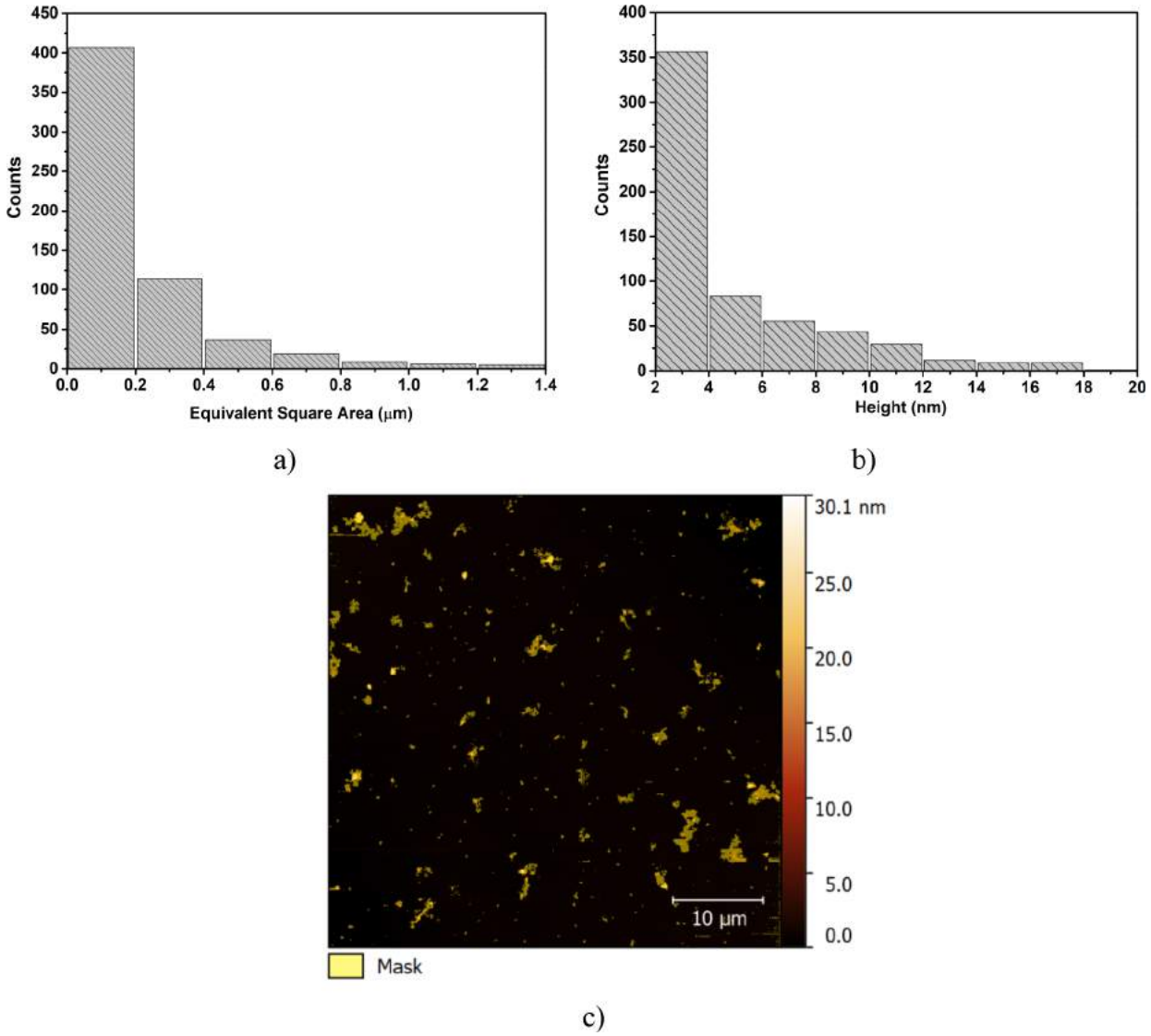

Figure 2. AFM analyses of multilayer graphene oxide (mGO) suspension: (a) lateral size measurements, (b) mGO flake heights, and (c) tomography image of mGO flakes (yellow regions).

histograms of lateral size and height generated by the topographic mapping obtained using AFM of mGO particles (after the exfoliation of GrO in a water medium). It is observed that most of the particles have an equivalent lateral size (Figure 2a) and height (Figure 2b) lower than 1.4 μm and 20 nm, respectively. Figure 2c shows an AFM image of mGO particles. This result evidences that the GO obtained has a few stacked layers after exfoliation, most probably below 25 layers, considering 0.78 nm for each layer.[38] This result shows that GO contains multilayers (mGO).

As seen in Figure 2c, the mGO nanoparticle has a very small size, and if these particles come into contact, the number of incommensurate contacts available to slip will also be very high, contributing to a strong lubricating effect.

From the standpoint of composites and nanocomposites, if particles agglomerate during melt mixing, countless out-of-register contacts may be present inducing the superlubricity phenomenon. Figure 3a,b shows an illustration of this phenomenon, which may justify the reduction of the storage and loss moduli and viscosity of composites obtained using the melt mixing method. In Figure 3a, the red and blue blocks represent two flake agglomerates (stacked). The θ symbol represents the orientations between the block of agglomerates in contact. This scheme could be used for Gr, GrO, and mGO particles. The agglomerate particles may stack in various angular orientations, in registry (commensurate contact), i.e., AB (0, 120, and 240° orientations) or AA (60, 180, and 300° orientations) stacking, and out of registry (incommensurate contact) (all the angular orientations are within 60° intervals). In Figure 3b, it can be observed that the atoms in the AB and AA stacking planes are perfectly aligned (in registry), and the slipping flake−flake contact presenting these orientations between planes occurs stick−slip friction.[31−34]

On the other hand, large contacts between flakes out of registry are also possible. All angular orientations between flake−flake contacts within the 60° interval are out of registry.[31−33] These angular orientations prevent a collective stick−slip motion between the interface atoms in contact during slipping.[31−34] The incommensurate contacts can also be noted in Figure 3b. The easy slipping of the incommensurate contacts present in the agglomerates may facilitate the polymer flow

DOI: 10.1021/acs.macromol.9b01746
Macromolecules 2019, 52, 9620−9631

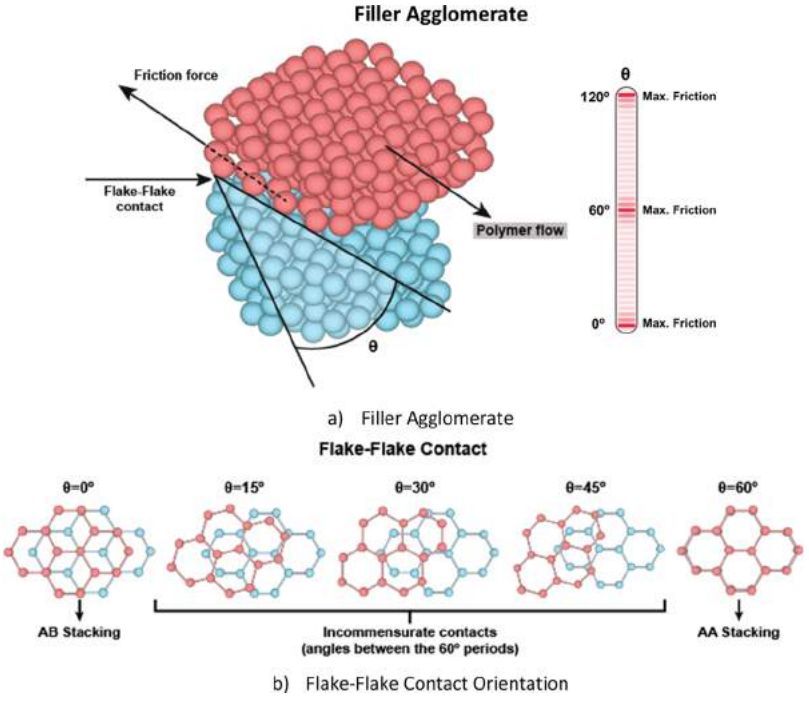

Figure 3. Superlubricity phenomenon of the agglomerates.(a) Filler agglomerate. (b) Flake−flake contact orientation.

when shear stress is applied, causing the viscosity and storage and loss moduli of the polymer to decrease.

Rheological Tests of Composites (HMWPE-Fillers and HDPE-Fillers). Taking into account the previous characterizations of the particles (Gr, GrO, and mGO), the rheological results of neat polymer and composites will be analyzed to understand the influence of the fillers on the flow behavior of the samples. Figure 4 shows the G', G'', and τ values versus the

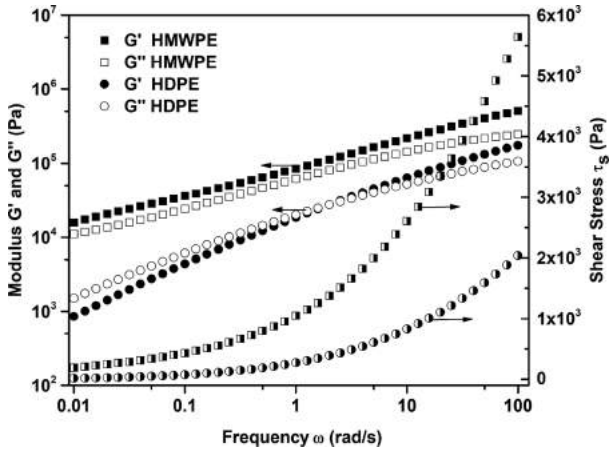

Figure 4. Storage (G') and loss (G'') moduli and shear stress (τ_s) of HDPE and HMWPE samples.

angular frequency of the polymers (HMWPE and HDPE). As can be seen in Figure 4, the modulus values (G' and G'') and the shear stress for HMWPE (range from 1.9×10^{-4} to 5.6×10^{-3} MPa) are higher than those for HDPE (range from 1.72×10^{-5} to 2.0×10^{-3} MPa) as expected. Polymers with high molecular weight present high values of modulus and shear stress due to the intense level of entanglements. Consequently, it is expected that the shear stress transferred from the HMWPE to the surface of fillers should also be higher than HDPE.

Figure 5a,b shows the storage modulus (G') and complex viscosity (η^*), respectively, of the composites (HMWPE-filler) produced by the insertion of Gr, mGO, and GrO (0.1 wt %). The storage modulus, G', and complex viscosity, η^*, are very sensitive when fillers are present to alter the polymer viscoelasticity, mainly at low frequencies with the rise of a "plateau" region for G', indicating a percolated network. Figure 5a shows the G' of HMWPE-fillers (0.1 wt %), and it is observed that the composites do not show a percolated network in the explored frequency range. Instead, the G' and η^* (Figure 5b) are reduced (at lower frequencies) by the insertion of 0.1 wt % of all fillers (Gr, GrO, and mGO). The same decrease is observed for the loss modulus, G'' (Figure 5S). This behavior is believed to occur due to the superlubricity effect of the agglomerated fillers described in the above section, which will improve the mobility of the molecular chains, leading to faster relaxation and low resistance to shear flow, as seen in Figure 5. However, other possibilities from the literature will be further discussed and disclosed for the work reported here.

It is important to highlight that the lowest interlayer shear strength measured for graphite (0.2 MPa), graphite oxide (2.1 MPa), and graphene oxide (0.46 GPa), as reported by Liu et al.,[19] Daly et al.,[20] and Wang et al.,[21] respectively, are at least hundred times greater than the transferred shear stress (range from 1.9×10^{-4} to 5.6×10^{-3} MPa) by the HMWPE and HDPE to fillers. Therefore, these rheological test conditions yield very low shear stress to overcome interlayer shear strength of the fillers.

Some publications have explained the decrease of the dynamic viscosity and modulus of polymers (ultrahigh-molecular-weight polyethylene (UHMWPE)[8] and polypropylene (PP)[9] due to the "selective adsorption" of chains with higher molar mass by filler, during crystallization (precipitation of larger chains) from the solution.[8,9] However, the chain length gradient at the filler surface is significantly lower or inexistent in the crystallization from melt when compared with the crystallization from solution. In this case, the selective adsorption as a justification for storage

DOI: 10.1021/acs.macromol.9b01746
Macromolecules 2019, 52, 9620−9631

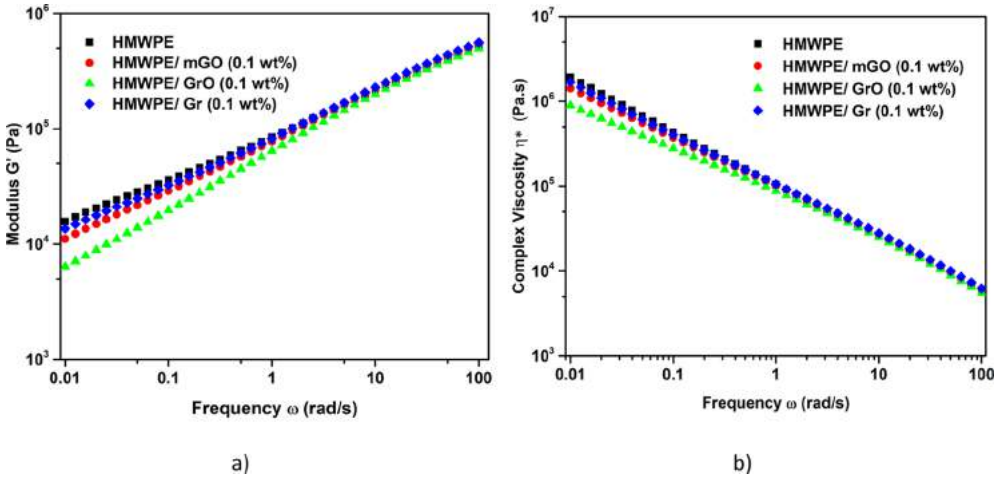

Figure 5. (a) Storage modulus and (b) complex viscosity of pure HMWPE and its composites containing 0.1 wt % mGO, GrO, and Gr.

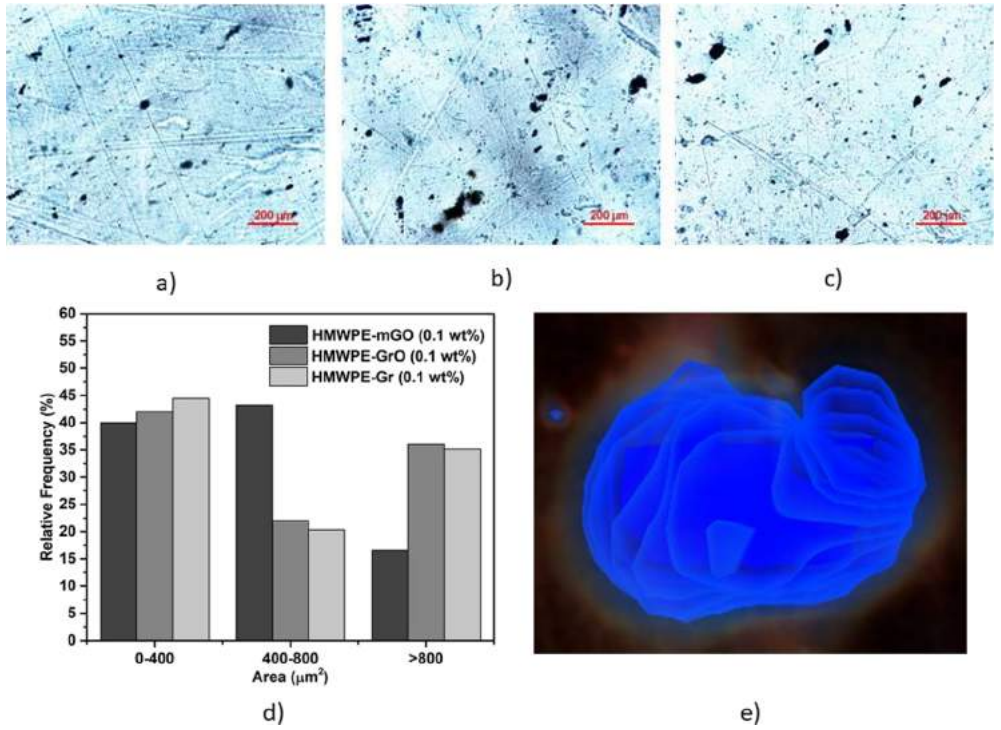

Figure 6. Optical images, size, and morphology of agglomerated fillers present in the HMWPE-fillers (0.1 wt %) composites. (a–c) Optical images of mGO, GrO, and Gr agglomerates obtained from optical micrography. (d) Agglomerate size obtained from optical images. (e) Images of mGO agglomerates present in composites obtained from X-ray microtomography analyses.

modulus and/or viscosity decrease is very unlikely since the composites were prepared using melt mixing. Bhusari et al. have attributed the reduction of η^* for the UHMWPE/HDPE blend with the addition of amino-functionalized GO and polyethylene modified with maleic anhydride to the physical plasticizing effect caused by short molecular chains of polyethylene grafted over GO.[16] Khasraghi and Rezaei have attributed the reduction of G' and η^* of UHMWPE/HDPE with the insertion of MWCNTs (1 wt %) to the entanglement molecule, reducing HDPE and UHMWPE phases due to the presence of the filler.[15] Both hypotheses used do not apply to our case.

Cho and Paul, on the other hand, attributed the reduction in the viscosity of nylon 6/organoclay nanocomposites to molecular degradation.[39] To verify whether the G', G'', and η^* reduction of the composites presented here are a result of molecular degradation, size exclusion chromatography analysis was used to measure the molecular weight and molecular distribution of the HMWPE and HMWPE-0.1 wt % filler composite samples tested using the oscillatory test. In the Supporting Information, Figure 6S and Table 1S, it is observed that the samples after the oscillatory test showed no significant difference between them in the number-average molecular weight ($\bar{M}_n$), weight-average molecular weight ($\bar{M}_w$), and polydispersity index (PDI). This indicates that the reduction of G' and G'' of the polymer is due to the intrinsic characteristics of the added fillers and not molecular degradation.

Therefore, it is expected that the dynamic rheological results observed for the HMWPE with 0.1 wt % filler content, presented in Figure 5, are due to the countless contacts out of registry present in the filler agglomerates, which allow the superlubricity

DOI: 10.1021/acs.macromol.9b01746
Macromolecules 2019, 52, 9620–9631

phenomenon to be observed. This mechanism induces the enhancement of molecular chain mobility and subsequently the decrease of storage modulus and complex viscosity. Figure 6 shows the optical images, size, and morphology of agglomerated fillers present in the HMWPE-filler (0.1 wt %) composites. In Figure 6a−c, the optical images of HMWPE containing mGO, GrO, and Gr are shown, respectively, obtained from optical micrography. It shows that all samples present filler agglomerates even when the composite is prepared using particles that have already been exfoliated (HMWPE-mGO). Figure 6d shows the histograms of agglomerate sizes of mGO, GrO, and Gr based on optical images. These histograms show that the HMWPE-Gr (0.1%) and HMWPE-GrO (0.1%) composites have the largest agglomerate areas, while nanoparticles of HMWPE-mGO (0.1%) form the smallest agglomerates. Therefore, mGO, even with lower agglomerates content, can support the lubricant effect.

Figure 6e shows an example of an agglomerate morphology of mGO contained in the HMWPE-mGO (0.1 wt%) composites observed for tomography. It shows that the flake agglomerates are stacked according to the illustration seen above (Figure 3). A large number of contacts out of registry are expected to be present in this agglomerate, inducing the filler superlubricity state during the composite rheological tests.[31,34] It is demonstrated that even two-dimensional fillers could lead to a lubricant effect on the polymer matrix since agglomerates are generated. It is very important to notice that the tomography resolution is only capable of identifying particles from micrometer- to macro-size dimensions (resolution of 2 μm/pixel); consequently, only agglomerates can be observed by the equipment used here.

The composites with Gr filler presented the smallest lubricant effect among fillers, followed by composites with mGO and GrO, as shown previously in Figure 5. The number of incommensurable contacts of the agglomerated GrO and mGO are greater than the Gr agglomerate. As previously discussed, the GrO filler has higher flake−flake contacts than Gr due to the strong fragmentation of graphite after oxidation. The larger number of flake−flake contacts of GrO explains the intensity of the lubricity behavior observed in the dynamic rheological results. Furthermore, GrO has more fault stacking,[40,41] decreasing, even more, the probability of AB restacking between flakes. mGO has a small lateral size and height (as seen in Figure 2), so the mGO agglomerates will also have a higher amount of incommensurable contacts than Gr. The presence of immeasurable contacts (different levels) justifies the lubrication intensity of the fillers for the HMWPE polymer, presented in the dynamic rheological measurements (Figure 5a,b).

It is important to note that the storage modulus of HMWPE with GrO has a significant value 75% lower than that with mGO, at a very low frequency (0.01 rad s^{-1}), despite the same chemical similarity between both fillers. The reason for this is that the HMWPE-mGO nanocomposite has a higher polymer-filler interphase contact and less flake−flake contact (agglomerate) than the HMWPE-GrO composite. This can be evidenced in Figure 7a,b, which displays the transmission micrograph images of HMWPE-mGO (0.1 wt %) and HMWPE-GrO (0.1 wt %) composites. Figure 7a shows an mGO nanoparticle (non-agglomerate) contained in the HMWPE-mGO (0.1 wt %) composite. This image indicates that some regions in the HMWPE-mGO (0.1 wt %) composite have not agglomerated but only present polymer-nanofiller contact. The image in Figure 7b shows a high amount of GrO agglomerate contained

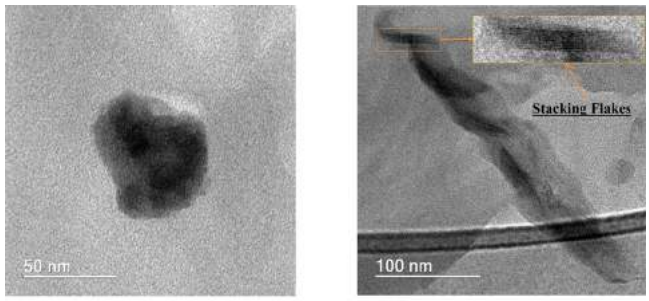

Figure 7. (a) TEM image of GO nanoparticle contained in the HMWPE-mGO (0.1 wt %) nanocomposites. (b) TEM image of GrO agglomerates contained in the HMWPE-GrO (0.1 wt %) composites.

in the HMWPE-GrO (0.1 wt %) composite. In this micrograph image, several stacking flakes are observed, as similarly observed for the mGO agglomerate in Figure 6e. As mentioned before, the easy slipping of the flakes present in the agglomerates promotes a lubricant effect, leading to a decrease in storage and loss moduli and complex viscosity, mostly due to the faster relaxation of molecular chains, as presented in Figure 5. This justifies the higher G' and η^* of the HMWPE-mGO nanocomposite in comparison to HMWPE-GrO since that presents a smaller amount of agglomerates.

To understand the relation between the number of agglomerates and the lubricant intensity of the fillers during the composite rheological tests, with the molecular weight of the polymers, a high filler content (5 wt %) was added to the HDPE and UHMWPE polymers to cause a drastic increase in agglomerated particles. Figure 8 shows the agglomerates of HMWPE and HDPE with 5 wt % content of fillers. A large and similar amount of agglomerates (black spots) in all the composites can be observed.

Figure 9a−d shows the results of the storage modulus and complex viscosity for (a, b) HMWPE composites and (c, d) HDPE composites with 5 wt % fillers in comparison with neat polymers. Note that when comparing the HMWPE-fillers (0.1 wt %) (Figure 5) with the HMWPE-fillers (5 wt %), an increase in filler content reduces the storage modulus and complex viscosity of the polymer, especially for GrO and mGO particles, for all frequencies (0.01−100 rad s^{-1}). The same behavior is observed for loss moduli, G'' (Figures 7S and 8S). This is attributed to the increase in incommensurate contacts by the high particle−particle interactions, and as was described above, will promote the lubricant effect of the particles, which during the flow will enhance the mobility of the molecular chains. The storage modulus and complex viscosity curves indicate that there is no significant difference between HMWPE composites prepared with mGO and GrO with 5% filler content, and their superlubricity effect to enhance chains relaxation is similar. This means that the GO particle agglomerates behave in a similar way to GrO particle agglomerates, relatively to their lubricant effect. However, when we compare HMWPE composites (Figure 9a,b) and HDPE composites (Figure 9c,d), it is noted there is a significant influence on the molecular weight, especially on storage modulus, with a more pronounced decreased for the HMWPE composites. This will be discussed in more detail below.

The molecular weight of the polymers (different transferred shear stresses) has a strong influence on the lubricant behavior of the agglomerated fillers. Figure 9c shows the storage modulus

DOI: 10.1021/acs.macromol.9b01746
Macromolecules 2019, 52, 9620−9631

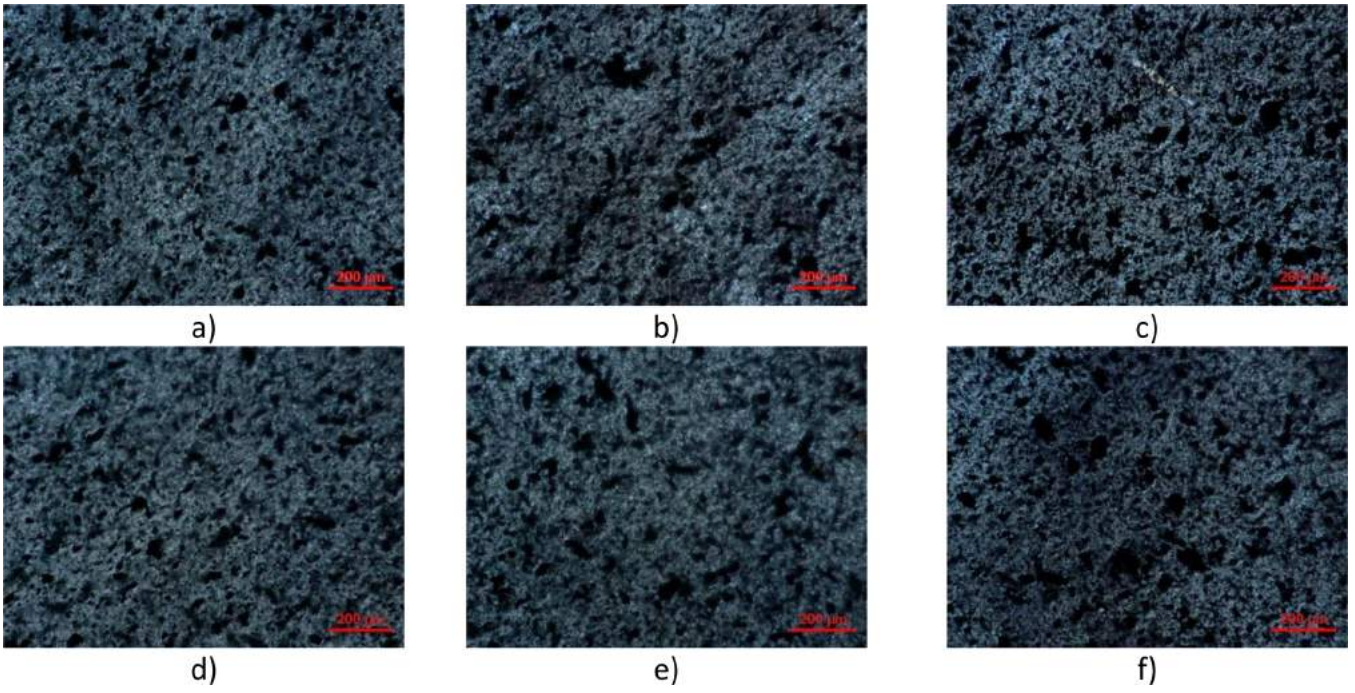

Figure 8. Optical micrograph images of (a) mGO, (b) GrO, and (c) Gr agglomerates containing HMWPE-fillers (5 wt %) and (d) mGO, (e) GrO, and (f) Gr agglomerates containing HDPE-fillers (5 wt %) composites.

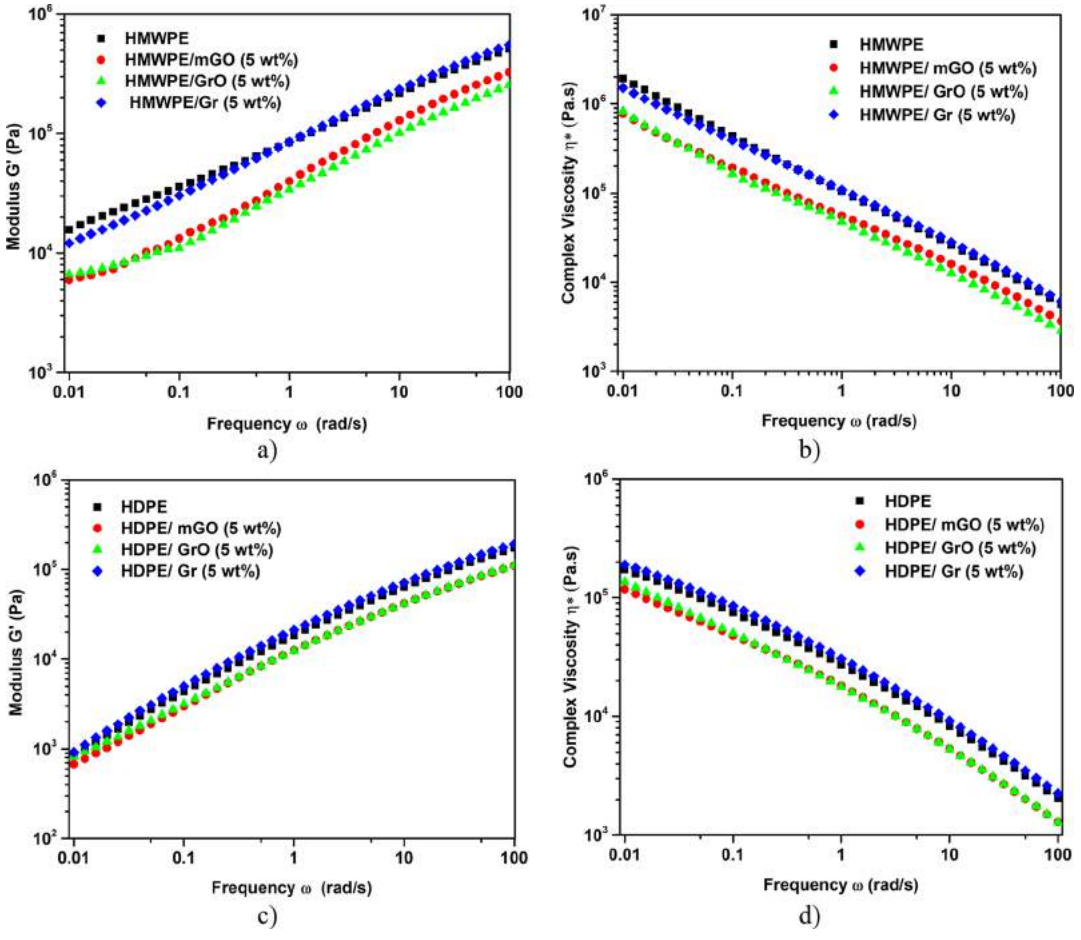

Figure 9. (a, c) Storage modulus (G') and (b, d) complex viscosity (η^*) of pure polymers and their composites with 5.0 wt % mGO, GrO, and Gr. (a, b) HMWPE and (c, d) HDPE.

DOI: 10.1021/acs.macromol.9b01746
Macromolecules 2019, 52, 9620−9631

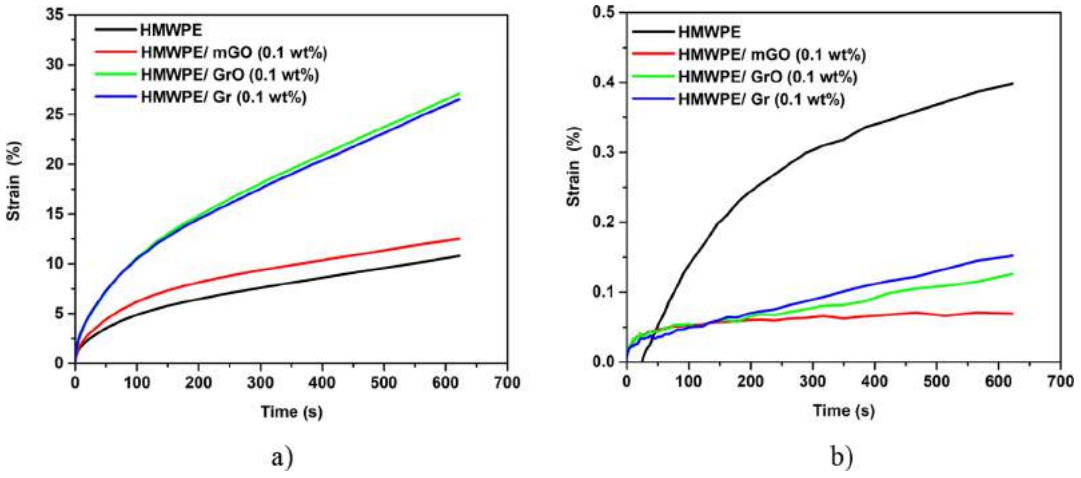

Figure 10. Strain of pure HMWPE and its composites containing 0.1 wt % Gr, GrO, and mGO during the creep test under a shear stress of (a) 5×10^{-4} MPa and (b) 1×10^{-5} MPa.

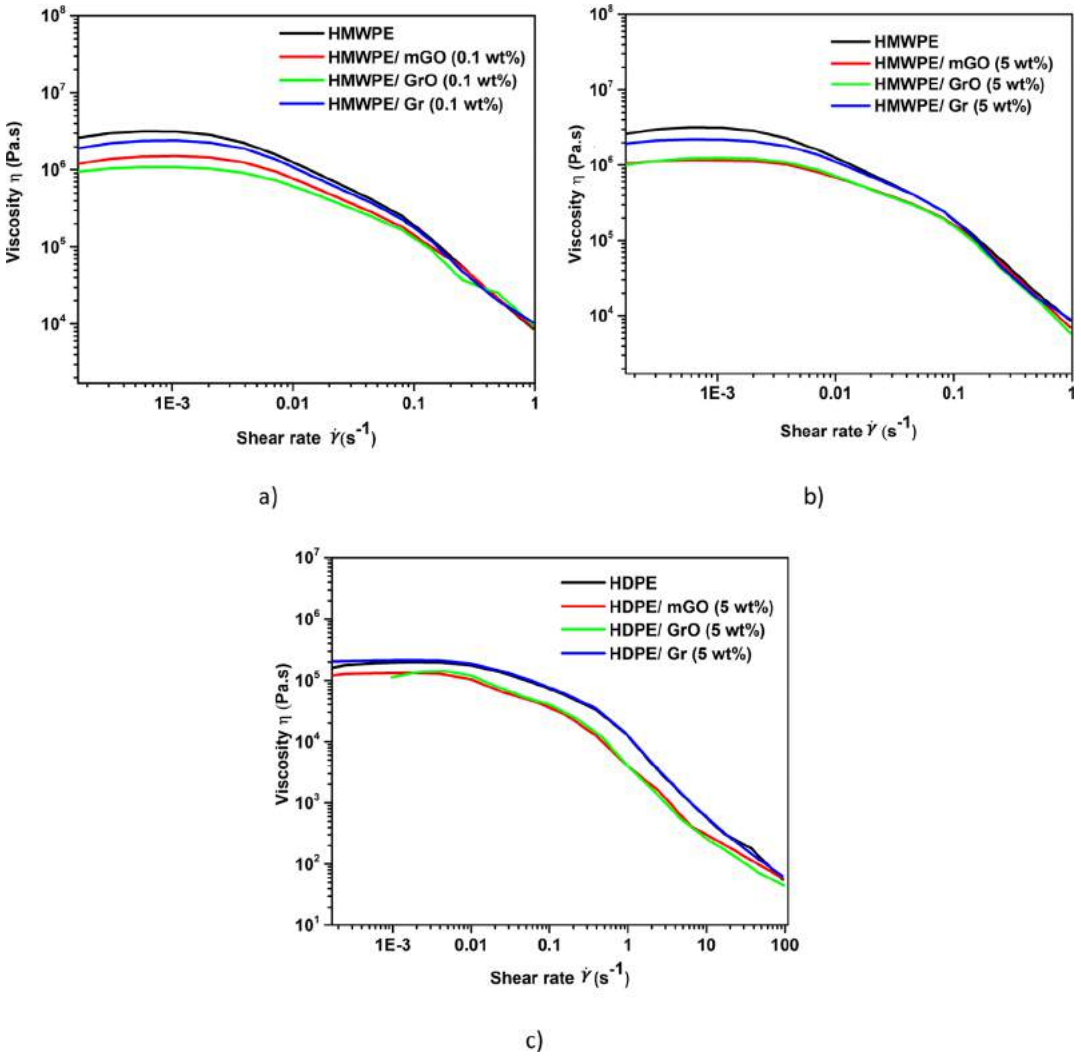

Figure 11. Log viscosity (η) vs log shear rate ($\dot{\gamma}$) of pure polymers and composites. (a) HMWPE-0.1 wt % (b) HMWPE-5.0 wt %, and (c) HDPE-5.0 wt %.

results for HDPE-fillers (5 wt %) composites. Remarkably, the presence of fillers in the HMWPE led to a less intense storage modulus than those inserted in HDPE. The same behavior is observed for loss moduli, G'' (Figures 7S and 8S). As seen in Figure 4, the HMWPE has higher transferred shear stress (τ) to the surface of the fillers than HDPE, causing larger slipping between the incommensurate contacts (flake−flake contacts). The G' curve of HDPE-Gr (5 wt %) composite overlapped the

DOI: 10.1021/acs.macromol.9b01746
Macromolecules 2019, 52, 9620−9631

curve of neat HDPE, which shows that the lubricant effect of graphite is not very noticeable. The same behavior is observed for loss moduli, G'' (Figure 8S). This is corroborated by Wu et al., who have also shown that the G' curve of HDPE with 2 and 6 wt % graphite overlapped the curve of neat HDPE.[18] The low shear stress transferred from HDPE to fillers and the few amounts of immeasurable contacts previously indicated for graphite agglomerates lead to no reduction in the storage modulus.

Dienwiebel et al. and Martin et al. have argued that in the "superlubricity state" for graphite and molybdenum disulfide, respectively, the friction is not completely absent but presents values very close to zero. To verify the dependence of the "superlubricity state" on fillers inserted in the polymer with applied shear stress, creep tests were performed under two shear stresses: one to induce (5×10^{-4} MPa) and one to avoid (1×10^{-5} MPa) the superlubricity phenomenon. Figure 10 shows the creep tests using HMWPE and 0.1 wt % filler as a standard sample. Note that both shear stresses applied are extremely lower than the interlayer shear strength of Gr, GrO, and mGO reported.[19−21] At 5×10^{-4} MPa of shear stress (Figure 10a), a stronger lubricant effect can be observed for composites with Gr and GrO, leading to higher deformations when compared with the neat polymer, whereas the composite with mGO only had a small increase in deformation. The slight increase in deformation can be associated with the slipping of the few mGO agglomerates present. On the other hand, nonagglomerated mGO particles hinder the relaxation of the polymer chain, reducing the deformation.

To avoid the "superlubricity state" of immeasurable contacts of the agglomerated fillers, shear stress very close to zero, 1×10^{-5} MPa, was applied. Figure 10b shows the deformation of the polymer and the composites under a shear stress of 1×10^{-5} MPa. In this condition, all fillers acted like stiff particles, reducing molecular mobility and deformation. All composites presented lower deformation than the neat polymer. The HMPWE-mGO (0.1 wt %) nanocomposites had the lowest deformation, and during the test, some samples did not deform.

The shear viscosity is strongly related to the polymer processability.[42] Polymers with high molecular weight are more difficult to process, reaching the extreme with very high molecular weight (1×10^6 to 6×10^6 g mol^{-1}) where the material becomes unprocessable by conventional methods (extrusion, injection, internal mixer, etc.).[43,44] Reducing the viscosity of the polymer by adding "processing aids" may allow the machine to operate at low energy consumption and high productivity.[42] Yip et al. and Kazatchkov et al. reported that platelet-like fillers, specifically boron nitride, can act as a processing aid, eliminating melt fracture and reducing the head pressure in the extrusion blow molding operation.[10,11]

To verify if the fillers (Gr, GrO, and mGO) can act as "processing aids" to the polyethylenes (HDPE and HMWPE), steady-state experiments were completed. This test is carried out under high shear rates allowing massive molecular disentanglement. The molecular disentanglement phenomenon is responsible for reducing the viscosity of the polymers becoming processable polymers. Steady shear viscosity (η) was measured during the test for HMWPE composites with 0.1 and 5 wt % filler and HDPE with 5 wt % filler as a function of the applied shear rate. Figure 11a−c shows the analysis of steady shear viscosity versus the shear rate of composites.

Two regions are observed in these images (Figure 11a−c). At a lower shear rate, up to ~2×10^{-3} s^{-1}, the polymer and the composites present a Newtonian behavior, called a Newtonian plateau. This means that the viscosity of the material is independent of the applied shear rate.[45] The low shear rate is insufficient to cause molecular disentangle, keeping the viscosity of the polymer constant. At a higher shear rate, shear-thinning behavior is observed (the second region observed). This means that the viscosity decreases with the increase in the shear rate. In this case, the applied shear rate is capable of causing molecular disentanglement, consequently reducing the viscosity of the polymer.[45] Aubry et al. define that at lower shear rates (Newtonian plateau), the behavior is governed by the influence of fillers in the system, while at higher shear rates (shear-thinning), the behavior is dominated by the polymer matrix.[46]

In Figure 11a,b, the results obtained agree with Aubry et al. In the region of the Newtonian plateau (low shear rate), usually associated with the molecule friction/hydrodynamic interactions, the HMWPE-filler (0.1 and 5 wt %) composites present viscosity lower than that of pure HMWPE, with the lubrication intensity of the fillers following the same lubricant order as the previous oscillatory tests. This is another indication that the fillers for the HMWPE are acting as lubricant particles by reducing the friction between molecules. At higher shear rates, the behavior is dominated by molecule disentanglement of the polymer matrix where the viscosity values of the composites and the polymers become very similar.

On the other hand, a polymer with a lower molecule entanglement density (HDPE), that is, lower molecular weight, the lubricant effect of the fillers can be observed in all ranges of the shear region, opposing Aubry et al. except for graphite, since it has fewer immeasurable contacts (Figure 11c). This leads to the indication that the lubricant effect of mGO agglomerates and GrO can also help the molecular disentanglement of polymers with low molecular weight even at higher shear rates. It is important to highlight again that the transferred shear stress (τ) from both polymers is only up to 2×10^{-2} MPa (see Figure 9S), significantly lower than the interlayer shear strength of fillers.[19−21] Once again, this result supports that the lubricant phenomenon observed is due to the "superlubricity state" of filler agglomerates and not attributed to the slip between the stacked layers that make up the filler structure.

The results observed in the steady-state regime lead to the conclusion that the superlubricity behavior of the fillers, mainly mGO and GrO agglomerates, can act as "processing aids" to the polyethylene of lower molecular weight, as is the case of the HDPE tested. Therefore, other rheological tests (capillary rheometers and torque rheometer) that allow higher shear rates to be applied, similar to the rates applied by the processing machines, are necessary to complement and validate such a hypothesis. This study will be developed in future work.

Generally, in composites, an increase in relaxation time means an interfacial interaction between the particles and the polymer matrix, which limits the mobility of polymer chains and increases the viscosity and moduli. With the aim to estimate the relaxation time (λ), the Carreau−Yasuda model was applied to the steady shear measurements. More details regarding the model and fitting can be found in the Supporting Information. Table 2S (Supporting Information) presents the λ of the HMWPE, HDPE, and their respective composites. By analyzing the HMWPE and its composites, a significant decrease in the λ for the composites can be clearly observed, indicating a faster relaxation of the polymer chains, especially for the GrO for 0.1 wt % and mGO for 5 wt %. These observations corroborate the previous comments, for the HMWPE composites, that filler

DOI: 10.1021/acs.macromol.9b01746
Macromolecules 2019, 52, 9620−9631

agglomerates present incommensurable contact, leading to easy slipping, which generates a lubricant effect. This phenomenon will mostly improve the molecular chain mobility of the HMWPE and consequently presents lower resistance to the shear flow. However, when the HDPE and its composites are analyzed, different results are seen. The λ increases for HDPE composites, when compared with HDPE, after the decrease in G', η^*, and shear viscosity are observed. It should be noted that the relaxation time is also affected by the polymer architecture (linear, branched, star, and ring), entanglement density, $\bar{M}_w$, and polydispersity; and for the case of the HDPE, a higher polydispersity than HMWPE is observed, which can affect the interaction between the fillers and the HDPE matrix differently and influence the relaxation time. To understand and have a complete picture of molecular dynamics of these composites, which was not the aim of this work, ideal monodisperse polymer matrices with specific architecture and different molecular weights should be used in future work.

CONCLUSIONS

Here, a study to understand the rheological behavior of polyethylene composites based on carbonaceous fillers was developed. Normally, it is expected that fillers must increase the storage modulus and viscosity of the polymer; however, the opposite behavior of carbonaceous fillers in the rheology properties of molten polymer matrices has been reported. Therefore, there are no coherent explanations around the real reason for the decrease of these rheological properties when the composites are prepared using melt mixing. The results show a large decrease in the storage modulus and viscosity of two different polyethylenes (molecular weight variation) with the addition of carbonaceous fillers: Gr, GrO, and mGO. It was shown that the shear stress and shear strain applied in the rheological tests are very low to overcome the interlayer shear strength of fillers. It is also very important to note that no significant molecular weight change was verified that justify the decrease of viscosity. Some observation could be extracted from the results obtained here:

I. The decrease of complex viscosity and storage modulus of composites is due to the increase of molecular chain mobility, based on the greater possibility of filler agglomerates presenting incommensurable contact leading to easy slipping, which generates a lubricant effect.
II. The lubricant effect of fillers observed here is attributed to the slipping of the agglomerates and not due to the interlayer shear strength being overcome since the shear stress needed for this is much higher than that applied during the rheological experiments, as shown.
III. The oxidation of graphite using Hummer's method caused strong fragmentation of graphite flakes creating various incommensurate contacts between agglomerates. This can explain the highest lubricity of GrO. The mGO, when it is well exfoliated in the polymer matrix, will not exhibit lubricant behavior. The presence of exfoliated mGO particles in the polymer increases the amount of mGO-polymer interphase, reducing the mobility chain and increasing the polyethylene viscosity and modulus. On the other hand, when mGO agglomerates are present, the flake−flake slipping promotes a reduction in the polymer modulus and viscosity.
IV. The "superlubricity state" was observed for all types of fillers inserted into two different polyethylenes when the rheological measurements were carried out at very low shear stress or shear strain. However, the lubricant effect vanishes when shear stress very near zero (1×10^{-5} MPa) was applied, confirming the supposition presented in "II" for the slipping of agglomerates.
V. In addition to the peculiarity of each filler, the lubricity intensity depends on the polymer molecular weight since polymers with higher molar weight transfer more shear stress to the filler surface during the oscillatory and steady shear experiments, which promotes larger agglomerate slipping.

ASSOCIATED CONTENT

Supporting Information

The Supporting Information is available free of charge at https://pubs.acs.org/doi/10.1021/acs.macromol.9b01746.

Filler characterization and also molecular weight measurements of HMWPE and its composites containing 0.1 wt % and aditional rheological data of polymer and their composites (oscilatory and steady state) (PDF).

AUTHOR INFORMATION

Corresponding Author

*E-mail: guilherminojmf@mackenzie.br.

ORCID

Guilhermino J. M. Fechine: 0000-0002-5520-8488

Notes

The authors declare no competing financial interest.

ACKNOWLEDGMENTS

The authors would like to acknowledge Fundação de Amparo a Pesquisa de São Paulo (FAPESP) for the grants 2012/50259-8, 2018/10910-8, and 2017/14640-2 and MackPesquisa (project number 181009) for the financial support. The authors also thank Braskem for the supply of polymers. The authors are grateful to Mrs. Camilla Thais de Meneses Landim for the graphic design of the images that describe the superlubricity phenomenon. We also acknowledge the Brazilian Nanotechnology National Laboratory (LNNano) for the X-ray Microtomography analysis. The study was also supported by the National Institute of Science and Technology of Carbon Nanomaterials of CNPq (INCT-Nanocarbono).

REFERENCES

(1) Thomas, S.; Muller, R.; Abraham, J. *Rheology and Processing of Polymer Nanocomposites*; John Wiley & Sons, Inc.: New Jersey, 2016.
(2) Jouault, N.; Vallat, P.; Dalmas, F.; Said, S.; Jestin, J.; Boué, F. Well-Dispersed Fractal Aggregates as Filler in Polymer−Silica Nanocomposites: Long-Range Effects in Rheology. *Macromolecules* **2009**, *42*, 2031−2040.
(3) El Achaby, M.; Qaiss, A. Processing and Properties of Polyethylene Reinforced by Graphene Nanosheets and Carbon Nanotubes. *Mater. Des.* **2013**, *44*, 81−89.
(4) Chaudhry, A.; Mittal, V. High-Density Polyethylene Nanocomposites Using Masterbatches of Chlorinated Polyethylene/Graphene Oxide. *Polym. Eng. Sci.* **2012**, *53*, 78−88.
(5) Song, Y.; Zheng, Q. Linear Viscoelasticity of Polymer Melts Filled with Nano-Sized Fillers. *Polymer* **2010**, *51*, 3262−3268.
(6) Einstein, A. Zur Theorie der Brownschen Bewegung. *Ann. Phys.* **1906**, *324*, 371−381.
(7) Mackay, M. E.; Dao, T. T.; Tuteja, A.; Ho, D. L.; van Horn, B.; Kim, H. C.; Hawker, C. J. Nanoscale Effects Leading to Non-Einstein-like Decrease in Viscosity. *Nat. Mater.* **2003**, *2*, 762−766.

DOI: 10.1021/acs.macromol.9b01746
Macromolecules 2019, 52, 9620−9631

(8) Zhang, Q.; Lippits, D. R.; Rastogi, S. Dispersion and Rheological Aspects of SWNTs in Ultrahigh Molecular Weight Polyethylene. *Macromolecules* **2006**, *39*, 658−666.
(9) Jain, S.; Goossens, J. G. P.; Peters, G. W. M.; van Duin, M.; Lemstra, P. J. Strong Decrease in Viscosity of Nanoparticle-Filled Polymer Melts through Selective Adsorption. *Soft Matter* **2008**, *4*, 1848−1854.
(10) Yip, F.; Diraddo, R.; Hatzikiriakos, S. G. Effect of Combining Boron Nitride With Fluoroelastomer on the Melt Fracture of HDPE in Extrusion Blow Molding. *J. Vinyl Addit. Technol.* **2000**, *6*, 196−204.
(11) Kazatchkov, I. B.; Yip, F.; Hatzikiriakos, S. G. The Effect of Boron Nitride on the Rheology and Processing of Polyolefins. *Rheol. Acta* **2000**, *39*, 583−594.
(12) Munoz, P. A. R.; de Oliveira, C. F. P.; Amurin, L. G.; Rodriguez, C. L. C.; Nagaoka, D. A.; Tavares, M. I. B.; Domingues, S. H.; Andrade, R. J. E.; Fechine, G. J. M. Novel Improvement in Processing of Polymer Nanocomposite Based on 2D Materials as Fillers. *Exp. Polym. Lett.* **2018**, *12*, 930−945.
(13) de Oliveira, Y. D. C.; Amurin, L. G.; Valim, F. C. F.; Fechine, G. J. M.; Andrade, R. J. E. The Role of Physical Structure and Morphology on the Photodegradation Behaviour of Polypropylene-Graphene Oxide Nanocomposites. *Polymer* **2019**, *176*, 146−158.
(14) Vega, J. F.; Martínez-Salazar, J.; Trujillo, M.; Arnal, M. L.; Müller, A. J.; Bredeau, S.; Dubois, P. Rheology, Processing, Tensile Properties, and Crystallization of Polyethylene/Carbon Nanotube Nanocomposites. *Macromolecules* **2009**, *42*, 4719−4727.
(15) Khasraghi, S. S.; Rezaei, M. Preparation and Characterization of UHMWPE/HDPE/MWCNT Melt-Blended Nanocomposites. *J. Thermoplast. Compos. Mater.* **2013**, *28*, 305−326.
(16) Bhusari, S. A.; Sharma, V.; Bose, S.; Basu, B. HDPE / UHMWPE Hybrid Nanocomposites with Surface Functionalized Graphene Oxide towards Improved Strength and Cytocompatibility. *J. R. Soc., Interface* **2019**, *16*, 20180273.
(17) Song, J.; Yang, W.; Fu, F.; Zhang, Y. The Effect of Graphite on the Water Uptake, Mechanical Properties, Morphology, and EMI Shielding Effectiveness of HDPE/Bamboo Flour Composites. *BioResources* **2014**, *9*, 3955−3967.
(18) Wu, G.; Lin, J.; Zheng, Q.; Zhang, M. Correlation between Percolation Behavior of Electricity and Viscoelasticity for Graphite Filled High Density Polyethylene. *Polymer* **2006**, *47*, 2442−2447.
(19) Liu, Z.; Zhang, S.-M.; Yang, J.-R.; Liu, J.-Z.; Yang, Y.-L.; Zheng, Q.-S. Interlayer Shear Strength of Single Crystalline Graphite. *Acta Mech. Sin.* **2012**, *28*, 978−982.
(20) Daly, M.; Cao, C.; Sun, H.; Sun, Y.; Filleter, T.; Singh, C. V. Interfacial Shear Strength of Multilayer Graphene Oxide Films. *ACS Nano* **2016**, *10*, 1939−1947.
(21) Wang, L.-F.; Ma, T.-B.; Hu, Y.-Z.; Wang, H. Atomic-Scale Friction in Graphene Oxide: An Interfacial Interaction Perspective from First-Principles Calculations. *Phys. Rev. B* **2012**, *86*, 1−9.
(22) Jeong, H.-K.; Lee, Y. P.; Lahaye, R. J. W. E.; Park, M.-H.; An, K. H.; Kim, I. J.; Yang, C.-W.; Park, C. Y.; Ruoff, R. S.; Lee, Y. H. Evidence of Graphitic AB Stacking Order of Graphite Oxides. *J. Am. Chem. Soc.* **2008**, *130*, 1362−1366.
(23) Krishnamoorthy, K.; Veerapandian, M.; Yun, K.; Kim, S. J. The Chemical and Structural Analysis of Graphene Oxide with Different Degrees of Oxidation. *Carbon* **2013**, *53*, 38−49.
(24) Duong, D. L.; Kim, G.; Jeong, H.-K.; Lee, Y. H. Breaking AB Stacking Order in Graphite Oxide : Ab Initio Approach. *Phys. Chem. Chem. Phys.* **2010**, *12*, 1595−1599.
(25) Vinod, S.; Tiwary, C. S.; Machado, L. D.; Ozden, S.; Cho, J.; Shaw, P.; Vajtai, R.; Galvão, D. S.; Ajayan, P. M. Strain Rate Dependent Shear Plasticity in Graphite Oxide. *Nano Lett.* **2016**, *16*, 1127−1131.
(26) Berman, D.; Erdemir, A.; Sumant, A. V. Graphene: A New Emerging Lubricant. *Mater. Today* **2014**, *17*, 31−42.
(27) Byun, I.-S.; Yoon, D.; Choi, J. S.; Hwang, I.; Lee, D. H.; Lee, M. J.; Kawai, T.; Son, Y.-W.; Jia, Q.; Cheong, H.; et al. Nanoscale Lithography on Monolayer Graphene Using Hydrogenation and Oxidation. *ACS Nano* **2011**, *5*, 6417−6424.
(28) Ko, J.-H.; Kwon, S.; Byun, I.-S.; Choi, J. S.; Park, B. H.; Kim, Y.-H.; Park, J. Y. Nanotribological Properties of Fluorinated , Hydrogenated , and Oxidized Graphenes. *Tribol Lett.* **2013**, *50*, 137−144.
(29) Hirano, M.; Shinjo, K. Superlubricity and Frictional Anisotropy. *Wear* **1993**, *168*, 121−125.
(30) Stankovich, S.; Dikin, D. A.; Piner, R. D.; Kohlhaas, K. A.; Kleinhammes, A.; Jia, Y.; Wu, Y.; Nguyen, S. B. T.; Ruoff, R. S. Synthesis of Graphene-Based Nanosheets via Chemical Reduction of Exfoliated Graphite Oxide. *Carbon* **2007**, *45*, 1558−1565.
(31) Dienwiebel, M.; Verhoeven, G. S.; Pradeep, N.; Frenken, J. W. M.; Heimberg, J. A.; Zandbergen, H. W. Superlubricity of Graphite. *Phys. Rev. Lett.* **2004**, *92*, 1−4.
(32) Dienwiebel, M.; Pradeep, N.; Verhoeven, G. S.; Zandbergen, H. W.; Frenken, J. W. M. Model Experiments of Superlubricity of Graphite. *Surf. Sci.* **2005**, *576*, 197−211.
(33) Verhoeven, G. S.; Dienwiebel, M.; Frenken, J. W. M. Model Calculations of Superlubricity of Graphite. *Phys. Rev. B* **2004**, *70*, 165418−165410.
(34) Liu, Z.; Yang, J.; Grey, F.; Liu, J. Z.; Liu, Y.; Wang, Y.; Yang, Y.; Cheng, Y.; Zheng, Q. Observation of Microscale Superlubricity in Graphite. *Phys. Rev. Lett.* **2012**, *108*, 205503.
(35) Martin, J. M.; Donnet, C.; Mogne, T. L.; Epicier, T. Superlubricity of Molybdenum Disulphide. *Phys. Rev. B* **1993**, *48*, 10583−10586.
(36) Falvo, M. R.; Steele, J.; Taylor, R. M.; Superfine, R. Gearlike Rolling Motion Mediated by Commensurate Contact : Carbon Nanotubes on HOPG. *Phys. Rev. B* **2000**, *62*, R10665.
(37) Pan, S.; Aksay, I. A. Factors Controlling the Size of Graphene Oxide Sheets Produced via the Graphite Oxide Route. *ACS Nano* **2011**, *5*, 4073−4083.
(38) Schniepp, H. C.; Li, J.-L.; Mcallister, M. J.; Sai, H.; Herrera-alonso, M.; Adamson, D. H.; Prud'homme, R. K.; Car, R.; Saville, D. A.; Aksay, I. A. Functionalized Single Graphene Sheets Derived from Splitting Graphite Oxide. *J. Phys. Chem. B* **2006**, *110*, 8535−8539.
(39) Cho, J. W.; Paul, D. R. Nylon 6 Nanocomposites by Melt Compounding. *Polymer* **2001**, *42*, 1083−1094.
(40) Pimenta, M. A.; Dresselhaus, G.; Dresselhaus, M. S.; Cançado, L. G.; Jorio, A.; Saito, R. Studying Disorder in Graphite-Based Systems by Raman Spectroscopy. *Phys. Chem. Chem. Phys.* **2007**, *9*, 1276−1290.
(41) Kumar; Pandian, R.; Das, P. K.; Ravindran, T. R.; Dash, S.; Tyagi, A. K. High-temperature phase transformation and low friction behaviour in highly disordered turbostratic graphite. *J. Phys. D: Appl. Phys.* **2013**, *46*, 395305.
(42) Murphy, J. *Additives for Plastics Handbook*; Second Edition, Elsevier Adcvanced Technology: New York, NY, 2001.
(43) Boscoletto, A. B.; Franco, R.; Scapin, M.; Tavan, M. An Investigation on Rheological and Impact Behaviour of High Density and Ultra High Molecular Weight Polyethylene Mixtures. *Eur. Polym. J.* **1997**, *33*, 97−105.
(44) González, J.; Rosales, C.; González, M.; León, N.; Escalona, R.; Rojas, H. Rheological and Mechanical Properties of Blends of LDPE with High Contents of UHMWPE Wastes. *J. Appl. Polym. Sci.* **2017**, *134*, 1−13.
(45) Barnes, H.; Hutton, J. K.; Walters, F. R. S. *An Introduction to Rheology*; First Edition, Elsevier Science Publishers, 1989.
(46) Aubry, T.; Razafinimaro, T.; Médéric, P. Rheological Investigation of the Melt State Elastic and Yield Properties of a Polyamide-12 Layered Silicate Nanocomposite. *J. Rheol.* **2005**, *49*, 425−440.

DOI: 10.1021/acs.macromol.9b01746
Macromolecules 2019, 52, 9620−9631